Change Detection of RSSI Fingerprint Pattern for Indoor Positioning System

Jaehyun Yoo, *Member, IEEE*

***Abstract*—A set of Wi-Fi RSSI (Received Signal Strength Indicator) measurements is one of basic sensory observation available for indoor localization. One major drawback of the RSSI based localization is maintenance of the RSSI fingerprint database, which should be periodically updated against measurement pattern changes caused by relocation, removal and malfunction of Wi-Fi APs (access points). To address this problem, a new change detection method is proposed in this paper. First, by machine learning techniques, the RSSI database is reconstructed to a probabilistic feature database by the implementations of PCA (Principal Component Analysis) and GP (Gaussian Process). Then, KL (Kullback-Leibler) divergence is used as a metric to measure the similarity of the existing database and a newly arrived test sets. The proposed method is evaluated by a real experiment at a multi-storey building. For experimental study, different cases that provoke changes of RSSI patterns are considered, and the positioning accuracy is examined by the *k*-NN (Nearest Neighbor) method. From the experimental results, it is found that the bigger the RSSI pattern changes, the large the KL divergences become. Also, when a modified change detection algorithm as the benchmark, which does not implement the PCA feature extraction, is compared, the proposed algorithm yields accurate and fast computing performances. In addition, the required number of survey points is empirically found associated with the threshold value to trigger the detection alarm.**

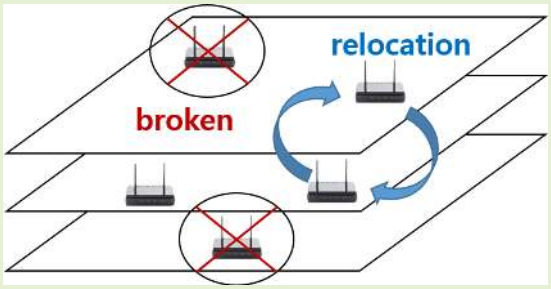

***Index Terms*— Wi-Fi RSSI fingerprint, indoor localization, feature extraction, machine learning, Gaussian process, KL divergence.**

I. Introduction

Wi-Fi RSSI based positioning [1]–[3] is one of standard approaches for indoor localization. It collects the complimentary Wi-Fi signals sent from a large number of APs that are already installed in indoor buildings. Regardless of private or public APs, their signals constitute a huge fingerprint database to mapping RSSI sets to locations. Due to its unbiased estimation capability, the Wi-Fi RSSI based localization is likely to be combined with other kinds of sensors such as IMU (Inertial Measurement Unit) [4], [5], camera [6], [7] and magnetic [8], [9].

One major drawback of the RSSI based approach is maintenance of the fingerprint database. The dimensionality of the RSSI set is defined as the number of APs that are scanned across the entire positioning field. Normally, the size of a Wi-Fi fingerprint database is so huge that consuming the considerable effort and resources for constructing and updating database are inevitable. Moreover, a study to recognize when we have to update the old database has not been enough addressed. Many APs used to be relocated, removed, and out of order. In these cases, the Wi-Fi RSSI pattern suddenly varies and the existing database does not fit a newly modified pattern.

To be robust to the environmental variation and to alleviate the effort for collection and calibration of the training data, many approaches have been suggested. Some works [10]–[12] propose to construct an alternative fingerprint map to replace the original RSSI fingerprint. In [10], the gradient fingerprints are made, and in [11], [12], the artificial fingerprints between labeled data points are estimated by the interpolation methods. The transfer learning, which identifies transfer knowledge of the localization models against the environmental variation over time and across space, has been applied for being adaptive localization [13]–[15]. The crowdsourcing is a strategy to exploit unlabeled data that include only RSSI measurements without the position labels. A huge amount of the unlabeled data can be easily collected inexpensively. In this context, the semi-supervised Laplacian learning [16]–[18] and semi-supervised deep learning [19]–[21] use the unlabeled data to improve the data efficiency without sacrificing the accuracy. The trajectory learning [22] to learn map information,

Manuscript received September 15, 2019; accepted October 27, 2019. Date of publication November 5, 2019; date of current version February 5, 2020. This work was supported by the National Research Foundation of Korea (NRF) Grant Funded by the Korean Government (MSIT) under Grant 2019R1F1A1057516. The associate editor coordinating the review of this article and approving it for publication was Prof. Okyay Kaynak.

The author is with the Department of Electrical, Electronic and Control Engineering, Hankyong National University, Anseoung 17579, South Korea (e-mail: jhyoo@hknu.ac.kr).

Digital Object Identifier 10.1109/JSEN.2019.2951712

the fusion with IMU (Inertial Measurement Unit) [23], and the probabilistic clustering [24] utilize also the crowdsourcing for the same purpose.

All of those methods focus on developing the positioning methods by leveraging some helpful models and crowdsourcing. However, they cannot help avoiding the degradation of accuracy by sudden and radical environmental changes such as the relocation of APs. This paper proposes a different aspect to prevent a loss of accuracy by suggesting a change detection algorithm to alarm to update the old database.

The main contribution of this paper is to develop a new change detection algorithm, which can recognize a rapid variation of the RSSI pattern and can decide when to update based on the analysis of the variation impact on the positioning accuracy. First, the original Wi-Fi RSSI dataset is transformed to a feature database by a feature extraction algorithm. It has been demonstrated from many works [22], [25]–[27] that the feature extraction method improve the localization accuracy. In this paper, the main reason for requiring the feature extraction is that the comparison between an original dataset and a test dataset becomes clearer on the feature space. For the purpose of the feature extraction, PCA (Principal Component Analysis) [28] is used to reduce the high dimensionality of the original RSSI fingerprint sets by eliminating the meaningless components in the data sets. Due to the data size reduction, the transformed feature database can reduce computation time significantly for change detection algorithm.

Second, Gaussian process [29] is applied to produce the likelihood distribution across physical space after the PCA implementation. The GP is one of machine learning algorithm, which estimates a target by means of probabilistic mean and variance. In this paper, by learning a relationship between the feature data produced by PCA and the positions, we can obtain the estimated distribution of the feature values across the entire interesting area. That is, the GP estimates can recover the region in which RSSI fingerprints are not observed. By the consecutive implementation of the PCA and the GP, a probabilistic fingerprint database is made to replace the original Wi-Fi RSSI fingerprint database.

Finally, the change detection algorithm based on information theory is suggested to derive a similarity between the existing database and a test set. KL divergence also known as the relative entropy [30] is a measure of the similarity between two probabilistic distributions, and it has been widely used in aspects of pattern recognition such as clustering, matching, and optimization [31]–[33]. For RSSI-based localization application, some works [33]–[35] also apply the KL (or Hölder) divergence to improve the positioning accuracy in clustering-based localization frameworks. In this paper, the KL divergence is used to find closeness between training database and test data set. Because the reconstructed database made by the PCA and GP algorithms is probabilistic, the KL divergence is a natural metric for the similarity judgement. When we set one density distribution from the reconstructed feature database and the other distribution as the test sets, the similarity can be calculated by the KL divergence. When the average of the KL divergences over some survey points (SP) exceeds a certain threshold, the change detection is triggered.

For evaluation of the proposed change detection algorithm, 2207 number of Wi-Fi RSSI training data and 204 number of test data from a multi-floor office building are collected. To evaluate the change detection performance, four different scenarios to provoke signal pattern variation are considered. The positioning is executed by the k-NN (Nearest Neighbor) method [36]. From the experimental results, it is found that the similarity metric decreases corresponding to the increment of the positioning error. The bigger the RSSI pattern changes, the larger the KL divergence becomes. Based on the analysis, the developed algorithm's accurate detection performance is validated. We additionally compare a modified change detection algorithm, which does not implement the feature extraction. The suggested algorithm yields more accurate and faster computing performances. Moreover, the required number of survey points is empirically found with respect to the threshold value to trigger the detection alarm.

The rest of this paper is as follows. Section II presents the Wi-Fi RSSI fingerprint reconstruction method by PCA and GP. Section III describes the change detection algorithm. Section IV and Section V report the experimental results and conclusion, respectively.

II. Probabilistic Fingerprint Database Reconstruction

Let us define N number of Wi-Fi RSSI fingerprint data sets in the following:

$$D = \{(\mathbf{x}_i, \mathbf{y}_i)\}_{i=1}^{N}, \tag{1}$$

where $\mathbf{x}_i$ and $\mathbf{y}_i$ are the i-th RSSI set and location, respectively. The i-th RSSI set $\mathbf{x}_i$ is composed of RSSI measurements, given by

$$\mathbf{x}_i = [x_i^1, x_i^2, \cdots, x_i^d]^T \in \mathbb{R}^d, \tag{2}$$

where x_i^j is the RSSI measurement between the j-th AP and the i-th receiver (e.g, a smartphone). The dimension of the RSSI data set equals to d number of APs scanned across the measurement collecting area. These data can be obtained by a single or multiple collectors. The i-th RSSI elements x_i^j for $j = 1, \cdots, d$ have the same received time-stamp. For $i \neq k \in \{1, \cdots, N\}$, the i-th and k-th data sets $\mathbf{x}_i$, $\mathbf{x}_k$ might have the same time-stamp. Nonetheless, they are treated as independent data sets, so time notation is omitted in this paper. The location $\mathbf{y}_i$ is given by

$$\mathbf{y}_i = [\mathrm{f}_i, \mathbf{p}_i]^T \in \mathbb{R}^3, \tag{3}$$

where f_i is a floor level and $\mathbf{p}_i$ is a 2-D position. In this paper, $\mathbf{p}_i$ is recorded by UTM (Universal Transverse Mercator) coordinate system. Later, the original database D will be transformed to a new feature database, given by:

$$F = \{(\mathbf{z}_i, \mathbf{y}_i)\}_{i=1}^{N}, \tag{4}$$

where $\mathbf{z}_i \in \mathbb{R}^r$ is a transformed feature set. The outstanding difference to the original database D is the much smaller dimensionality than the original one, i.e., $r \ll d$.

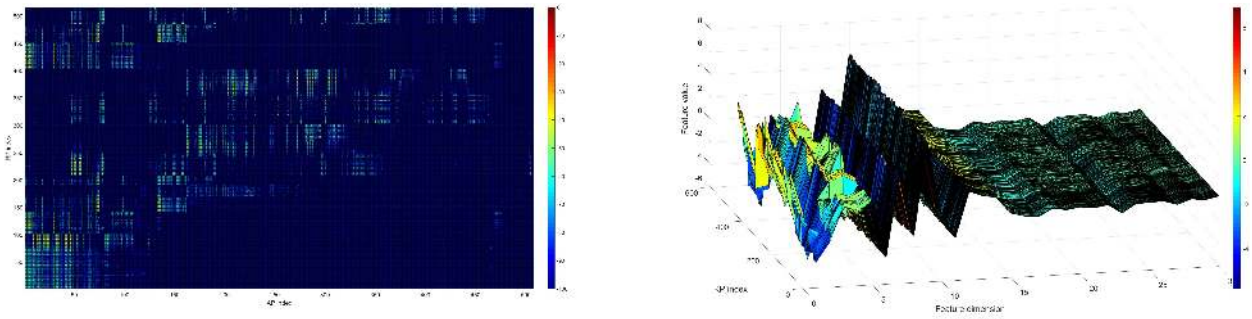

(a) Original Wi-Fi RSSI database

(b) PCA-transformed database

Fig. 1. In (a), the original Wi-Fi RSSI distribution of the training database is shown where x-axis and y-axis indicate the AP (Access Point) and RP (Reference Point) indices, respectively. The distribution in (a) shows how much sparse the raw Wi-Fi RSSI fingerprints are, where there are too many slots having -100 dBm as the value of the possibly smallest value. In (b), the transformed database made by PCA. The feature distribution is drawn along the transformed feature dimension instead of AP index. The feature influence appears until the 20-th feature dimension since the feature values after the 20-th dimension are biased to zero.

The rest of this section will describe how to construct the feature database by the PCA in Section II-A and the GP in Section II-B.

A. PCA

PCA (principal component analysis) is an unsupervised learning method and it does not need labels of input data, e.g., locations.

By the PCA, the transformation from the original dataset $\mathbf{x}_i$ to the feature dataset $\mathbf{z}_i$ is executed by the matrix $\mathbf{P}$ in the following:

$$\mathbf{z}_i = \mathbf{P}^T \mathbf{x}_i. \tag{5}$$

To find $\mathbf{P}$, the PCA solves a generalized eigenvalue problem. Let $\{\rho_i\}_{i=1}^d$ be the generalized eigenvectors associated with the generalized eigenvalues $\{\lambda_i\}_{i=1}^d$ of the following generalized eigenvalue problem:

$$\mathbf{A}\rho_i = \lambda_i \mathbf{I}\rho_i, \quad i = 1, \ldots, d, \tag{6}$$

where $\mathbf{I}$ is an identity matrix and $\mathbf{A}$ is a scatter matrix, given by:

$$\mathbf{A} = \sum_{i=1}^{N} (\mathbf{x}_i - \mu)(\mathbf{x}_i - \mu)^T, \tag{7}$$

with the mean of all the RSSI samples μ:

$$\mu = \frac{1}{N} \sum_{i=1}^{N} \mathbf{x}_i. \tag{8}$$

Then, the transformation matrix $\mathbf{P}$ is obtained by solving the following optimization problem:

$$\mathbf{P} = \text{argmax}_{\mathbf{P}} \frac{|\mathbf{P}^T \mathbf{A} \mathbf{P}|}{|\mathbf{P}^T \mathbf{I} \mathbf{P}|}. \tag{9}$$

The condition of the eigenvalue problem is as follows. The generalized eigenvectors are orthogonal:

$$\rho_i^T \rho_j = 0, \quad \text{for } i \neq j, \tag{10}$$

and the generalized eigenvectors are normalized:

$$\rho_i^T \rho_i = 1, \quad \text{for } i = 1, \ldots, d. \tag{11}$$

When the eigenvalues are sorted in descending order:

$$\lambda_1 \geq \lambda_2 \geq \cdots \geq \lambda_d, \tag{12}$$

the transformation matrix P is obtained by:

$$\mathbf{P} = \left(\sqrt{\lambda_1}\rho_1 | \sqrt{\lambda_2}\rho_2 | \cdots | \sqrt{\lambda_r}\rho_r \right). \tag{13}$$

From (13), we can figure out that the influence of the transformation becomes weaker as the dimensionality order increases, because the values of eigenvalues and eigenvectors decreases according to the dimensionality increment.

Fig. 1 shows the original Wi-Fi RSSI distribution and the PCA-driven feature distribution. In Fig. 1(a), the original database suffers from the sparsity in which many slots on the AP (Access Point) indices on x-axis and RP (Reference Point) indices on y-axis are filled with the possibly lowest value -100 dBm. Because one AP can cover only small area relative to the entire positioning field, the majority of the elements in the RSSI vector in (2) are rarely filled with some meaningful values between 0∼-60 dBm. In Fig. 1(b), those useless elements dominated by -100 dBm values are filtered out as a result of the PCA transformation. The important features appear at the front part on the feature dimension (see 0∼20-th feature dimension on x-axis). This can be confirmed by the PCA equation in (13). The feature data after the 20-th feature dimension lose their influence because they are almost biased to zero.

Given the PCA-transformed database as shown in Fig. 1(b), the following section introduces the next step to complete the reconstruction of the RSSI fingerprint database.

B. GP (Gaussian Process)

The GP seeks to find a hidden posterior distribution over functions $g(\cdot)$ from training data $F = \{(\mathbf{z}_i, \mathbf{y}_i)\}_{i=1}^N$ defined in (4) under the assumption of

$$\mathbf{z}_i = g(\mathbf{y}_i) + \varepsilon,$$

where the noise ε follows the Gaussian distribution $\mathcal{N}(0, \sigma_{GP}^2)$ with zero mean and variance σ_{GP}^2. A key idea underlying GP is the requirement that the function values at different data points are correlated, where the covariance between two

function values $g(\mathbf{y}_i)$ and $g(\mathbf{y}_j)$ depends on the inputs $\mathbf{y}_i$ and $\mathbf{y}_j$. This dependency can be specified via the Gaussian kernel function $k(\mathbf{y}_i, \mathbf{y}_j)$, given by

$$k(\mathbf{y}_i, \mathbf{y}_j) = \theta_1 \exp\left(\frac{-\parallel \mathbf{y}_i - \mathbf{y}_j \parallel^2}{2\theta_2}\right), \tag{14}$$

where the hyper-parameters θ_1 and θ_2 represent a smoothness of the function estimated by the GP.

According to the GP, the joint distribution over the training outputs $\mathbf{Z} = [\mathbf{z}_1, \cdots, \mathbf{z}_N]$ is a function of the training inputs $\mathbf{Y} = [\mathbf{y}_1, \ldots, \mathbf{y}_N]^T$, where $\mathbf{z}_i$ is a feature value at the interested location $\mathbf{y}_i$, given by:

$$\mathbf{Z} \sim N\left(0, K(\mathbf{Y}, \mathbf{Y}) + \sigma_{GP}^2 I\right), \tag{15}$$

where $K(\mathbf{Y}, \mathbf{Y})$ is an $N \times N$ kernel matrix whose (i, j)-th element is $k(\mathbf{y}_i, \mathbf{y}_j)$ in (14).

In this paper, the GP is used to estimate the feature distribution over the workspace by setting the input $\mathbf{y}*$ as the every location grid. The estimate consists of the mean $\mu_{\mathbf{y}_*}$ and the variance $\sigma^2_{\mathbf{y}_*}$, given by:

$$p\left(g(\mathbf{y}_*)|\mathbf{y}_*, \mathbf{Y}, \mathbf{Z}\right) = N\left(\mu_{\mathbf{y}_*}, \sigma^2_{\mathbf{y}_*}\right),$$

and

$$\mu_{\mathbf{y}_*} = \mathbf{k}_*^T \left(K(\mathbf{Y}, \mathbf{Y}) + \sigma_{GP}^2 I\right)^{-1} \mathbf{Z} \tag{16}$$

$$\sigma^2_{\mathbf{y}_*} = \mathbf{k}(\mathbf{y}_*, \mathbf{y}_*) - \mathbf{k}_*^T \left(K(\mathbf{Y}, \mathbf{Y}) + \sigma_{GP}^2 I\right)^{-1} \mathbf{k}_*, \tag{17}$$

where $\mathbf{k}_*$ is the $N \times 1$ vector referring to covariances between a test set $\mathbf{y}_*$ and the training input data $\mathbf{Y}$. The mean values represent the predicted feature values for newly coming RSSI measurements at a certain position. The GP outcomes will be used to detect change of the RSSI pattern, which will be introduced in the next section.

III. Change Detection by KL Divergence

The KL divergence is defined as a measure of difference between two probability density functions $f(\mathbf{y})$ and $h(\mathbf{y})$:

$$KL(f||h) \triangleq \int f(\mathbf{y}) \log \frac{f(\mathbf{y})}{h(\mathbf{y})} dy. \tag{18}$$

In the case of both $f(\mathbf{y})$ and $h(\mathbf{y})$ are Gaussian distribution, the KL divergence is of the form

$$KL(f||h) = \frac{1}{2}\Big(\mathrm{tr}(\Sigma_h^{-1}\Sigma_f) - r + \ln\frac{|\Sigma_h|}{|\Sigma_f|} + (\mu_h - \mu_f)^T \Sigma_h^{-1}(\mu_h - \mu_f)\Big), \tag{19}$$

where r is the dimensionality of the feature set, μ and Σ are the mean and variance of a Gaussian distribution. In our application, $f(\mathbf{y})$ is defined as the distribution of the the training database calculated by the GP, while $h(\mathbf{y})$ is the approximation by the GP estimation for the test sets.

To detect the change of the RSSI pattern over the workspace, we need to designate some position points preliminarily to survey the signal variation. This paper call these points SPs (Survey Points) as shown in Fig. 2. Let us define Y_{survey} as the set of m number of the survey points:

$$Y_{\text{survey}} = \{\mathbf{y}_1^*, \mathbf{y}_2^*, \ldots, \mathbf{y}_m^*\}, \tag{20}$$

where the position label $\mathbf{y}_j^*$ has the same form of (3). By using the training data with GP implementation (16) and (17), the reconstructed feature set at each $\mathbf{y}_j^*$ can be defined as

$$Y_{\text{SP}}^* = \left\{(\mu_{\mathbf{y}_1^*}, \sigma_{\mathbf{y}_1^*}), \cdots, (\mu_{\mathbf{y}_m^*}, \sigma_{\mathbf{y}_m^*})\right\}. \tag{21}$$

We note that the feature sets Y_{SP}^* at every survey point are obtained once in the offline phase. Each set of $(\mu_{\mathbf{y}_i^*}, \sigma_{\mathbf{y}_i^*})$ is used to calculate $f(\mathbf{y}_i^*)$ for the KL divergence. Fig. 2 illustrates the production of Y_{SP}^* with the GP.

Similarly, suppose a test set Y_{tst}^* is given by an examiner who collects new RSSI measurement sets at the SPs. Then, by using Y_{tst}^* to calculate $h(\mathbf{y}_{tst}^*)$, we can obtain (19) at a SP. Then, the average of the KL divergences at all SPs is calculated and can be used for the change detection.

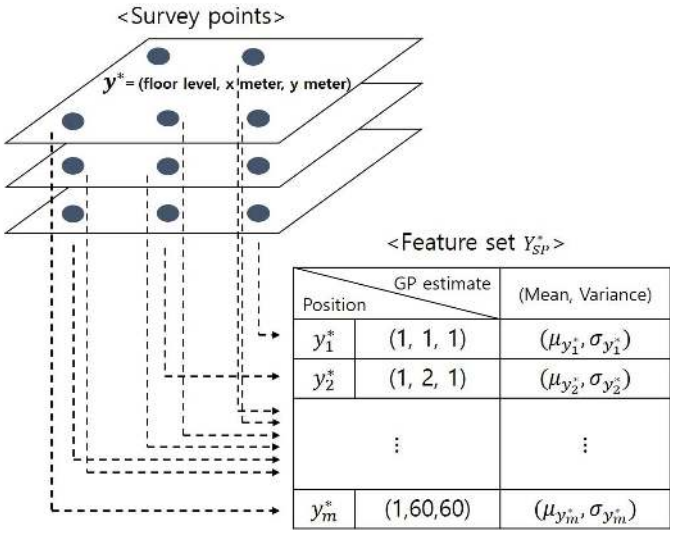

Fig. 2. The description of a feature database Y_{SP}^* by GP estimates on SPs (Survey Points). The number of the SPs would be smaller than the RPs (Reference Points) at which all training data points are collected. The location consists of (floor level, x meter, y meter), where 2D position is recorded as the UTM (Universal Transverse Mercator) coordinate system. The feature values including mean and variance are the results of the GP estimation as in (16) and (17).

IV. Experimental Results

For experimental study, we collect the Wi-Fi RSSI data from a multi-story office building. Total 2207 number of training data points and 204 number of test data points are used, and 508 number of different AP devices is scanned. The original data dimensionality is 508, i.e. $d = 508$, and the reduced dimensionality is set 10, i.e. $r = 10$. The RPs at which trainers record the RSSI measurements and positions are designated preliminarily on 1×1 m^2 grid. Also, 100 number of SPs are used for the change detection evaluation. The used training data and SPs are illustrated in Fig. 3(d).

To test positioning accuracy, we perform position estimation by k-NN method. The k-NN is one of standard positioning

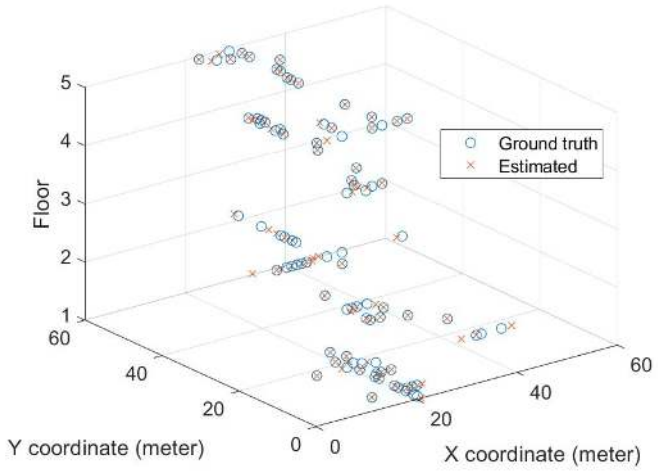

(a) Normal data, ave.error=0.7975 m

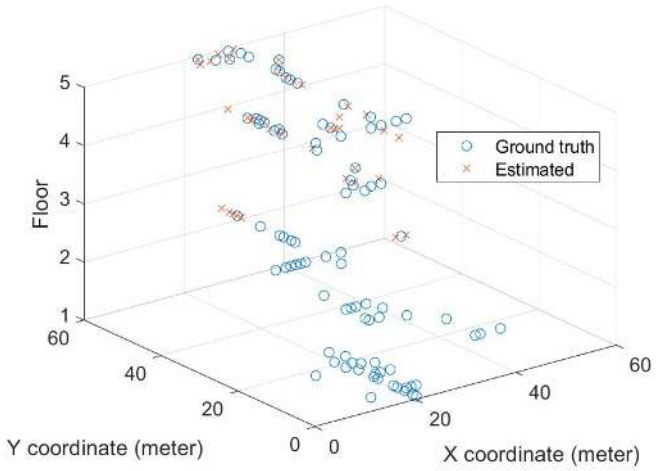

(b) Polluted data by Case 1, ave.error=22.5106 m

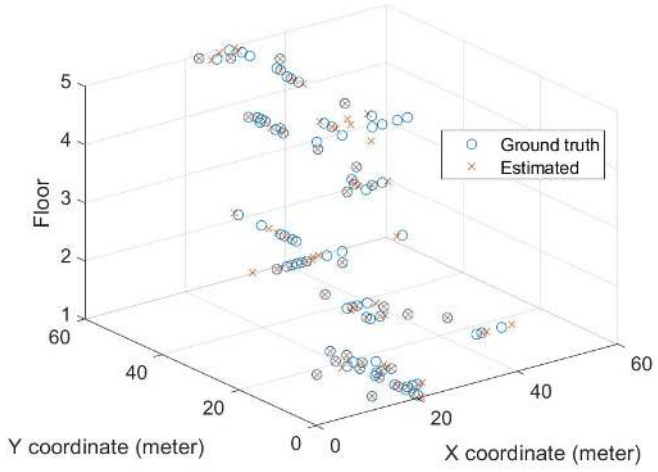

(c) Polluted data by Case 2, ave.error=1.3106 m

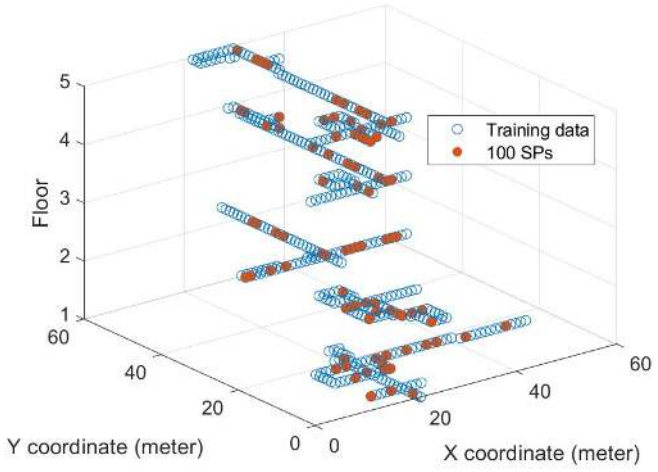

(d) Training data and survey points

Fig. 3. Positioning results by k-NN with $k = 2$ when using three different test data sets, where (a): original test data, (b): severely polluted test data by Case 1 and (c): minorly polluted test data by Case 2. In (d), the training data and survey points are illustrated.

algorithm, which selects k number of the points in the training database nearest to a test measurement. Then, it decides the estimated position by averaging the selected positions. The position error is defined as the average of norm. For the positioning, $k = 2$ is determined after tuning for best performance.

To make radical changes to the RSSI pattern, we consider 4 different cases belonging to 2 individual scenarios:

- Scenario 1: Switch some APs' locations with some APs' locations.
  - Case 1: APs to be switched are important.
  - Case 2: APs to be switched are not important.
- Scenario 2: Remove some APs.
  - Case 3: APs to be removed are important.
  - Case 4: APs to be removed are not important.

Scenario 1 considers when the locations of two groups of APs are switched. Scenario 2 refers to when some APs are removed or broken. For that, the values obtained from those APs are preset to the possibly minimum value -100 dBm. The important APs generate meaningful RSSI and play a pivotal role in localization. Although the true locations of the 508 APs are not known in the experimental site, we can infer which APs are more important than the others. In Fig. 1(a), certain meaningful RSSI values (between 0∼-60 dBm) are recorded on the indices of the important APs, whereas almost -100 dBm values are stamped along the indices of the majority of the unimportant APs. For Case 1, 1∼101th APs on the dimensionality indices are switched with 401∼501th APs. For Case 2, 350∼399th APs are switched with 400∼499th APs. For Case 3, 1∼50th APs are removed. For Case 4, 450∼499th APs are removed. It is noted that investigating the situation for *randomly* selected APs is not helpful for the analysis because the corresponding result is dependent on how many important APs are included in the random selection.

Fig. 3 shows three positioning results. Fig. 3(a) is the result when using the normal test data set. Fig. 3(b) is the result when testing the severely polluted data set followed

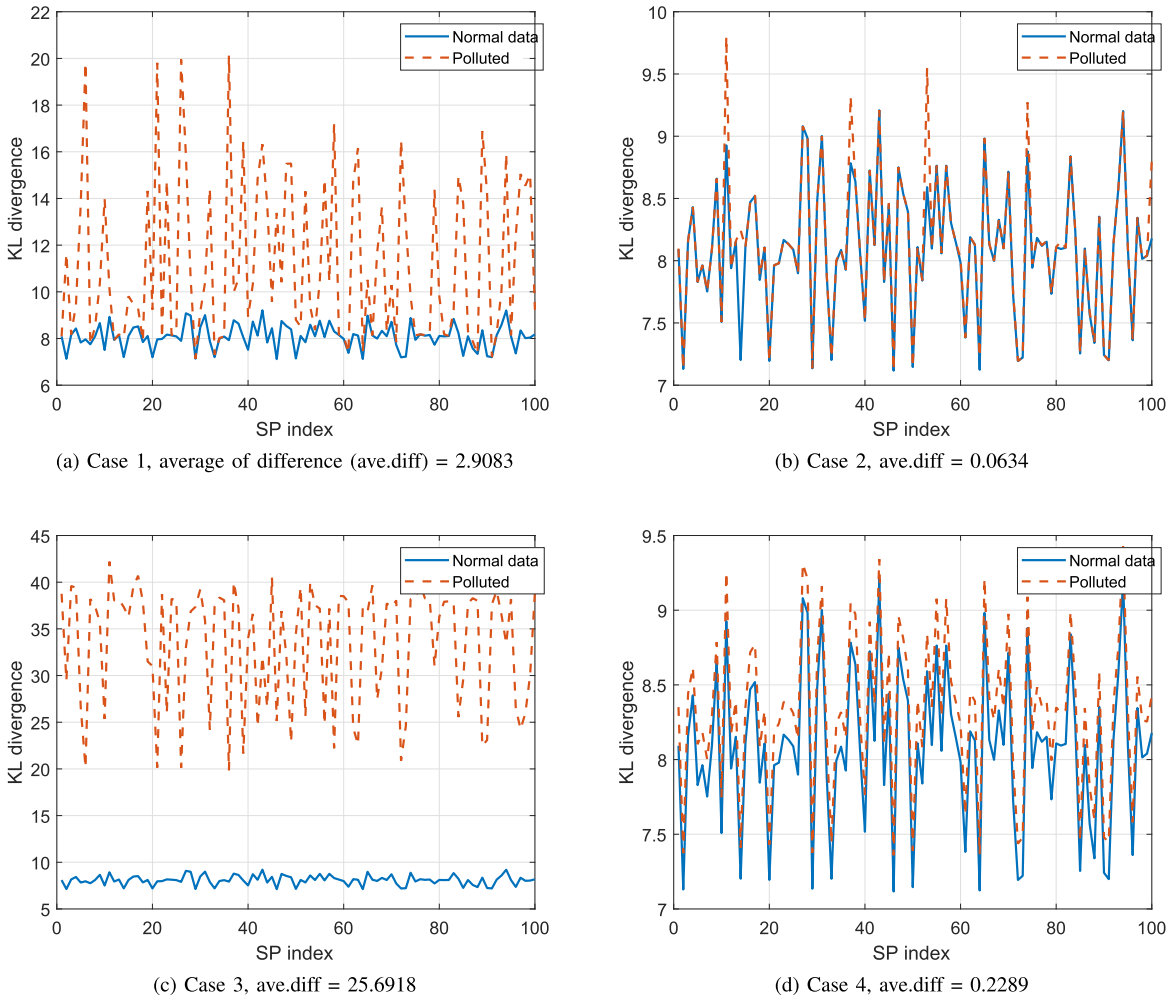

(a) Case 1, average of difference (ave.diff) = 2.9083

(b) Case 2, ave.diff = 0.0634

(c) Case 3, ave.diff = 25.6918

(d) Case 4, ave.diff = 0.2289

Fig. 4. Experimental results of the KL divergence between the normal test data and the polluted data sets made by rule of Case 1∼4. The outstanding differences are found in (a) and (c) due to the big change of the RSSI pattern, whereas the trivial differences appear in (b) and (d) by the minor change. We can make a simple detection alarm logic such as 'detect if ave.diff $>$ 1.5'. With this setup, it can detect the change that causes the significant localization error such as Case 1 in Fig. 3(b) while allowing the trivial localization loss such as Case 2 in Fig. 3(d).

by Case 1, and Fig. 3(c) is the result when the minorly polluted test data set by Case 2. As shown in Fig. 3(a), when a test set comes from the same RSSI distribution of the existing database, it yields high accuracy. However, as shown in Fig. 3(b), when a test set is distorted by the environmental change of RSSI pattern, the accuracy significantly decreases. In Fig. 3(c), the localization can still hold small error when the RSSI pattern is minorly changed. The average positioning errors for each Cases 1∼4 are 22.5 m, 1.3 m, NaN, 2.7 m, respectively, where NaN refers to the tremendous error due to wrong floor level estimation.

Fig. 4 shows the results of the KL divergence between the test data and the polluted data sets produced by Case 1∼4. The RSSI changes with respect to the modification of the important APs following Case 1 and Case 3 cause the large distinctions of the KL divergence as shown in Fig. 4(a) and 4(c). On the other hand, Fig. 4(b) and 4(d) do not indicate outstanding difference of KL divergence due to the minor RSSI changes following Case 2 and Case 4. By defining a threshold ($\approx$ 1.5 in this paper) on the average of KL divergence, we can determine the detection alarm moment.

The proposed change detection method consists of the PCA feature extraction, GP learning and KL divergence. Among these, the PCA feature extraction could be theoretically optional for completing the change detection algorithm. To investigate the effect of the feature extraction, we revise the proposed change detection method by extracting the PCA feature extraction from the original change detection algorithm. Fig. 5 shows the KL divergence results of the modified algorithm according to the four cases under the same experimental setup as in Fig. 4. The result of this modified method is not accurate because the minor-variation by Case 4 has large KL divergence difference (compare the difference of Fig. 4(d) and Fig. 5(d)), which leads the false detection alarm. In addition, without the feature extraction, much computation time is required as summarized in TABLE I, because it needs the $d = 508$ number of GP executions, whereas the proposed method consumes only $r = 10$ GP executions. As a result,

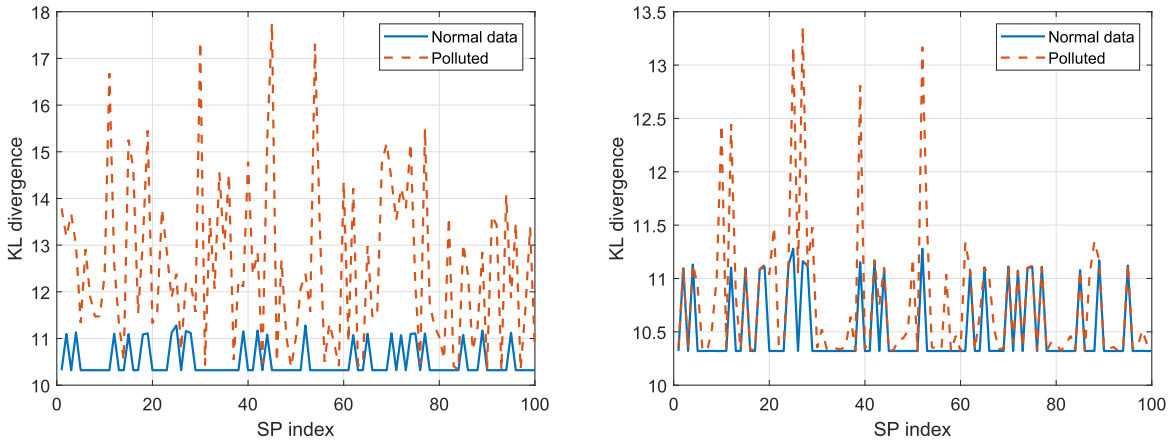

(a) Case 1, ave.diff = 2.0236

(b) Case 2, ave.diff = 0.2684

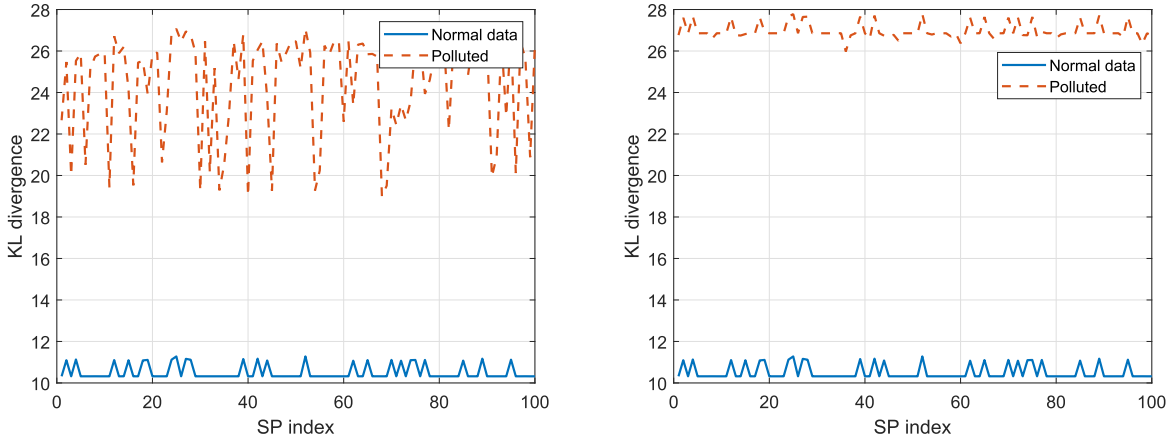

(c) Case 3, ave.diff = 13.9198

(d) Case 4, ave.diff = 16.4455

Fig. 5. The performances of the modified change detection method that does not implement the PCA feature extraction are shown under the same experiment setup to Fig. 4. This compared algorithm cannot distinguish the AP variation situation because the minor change in (d) Case 4 has large KL divergence values, which causes a fault detection alarm.

TABLE I
COMPUTATION TIME (SEC)

	Case 1	Case 2	Case 3	Case 4
Proposed change detection	1.45	1.33	1.27	1.37
Compared change detection	26.15	25.51	25.73	25.59

in terms of the accuracy and computation efficiency, the PCA-based feature extraction is functionally essential for the change detection algorithm.

Finally, we additionally investigate the effect of the number of SPs on the change detection mechanism. In the primary results shown in Fig. 4, the 100 SPs as illustrated in Fig. 3(d) are used in which the change detection was perfectly performed. To vary the number of SPs, ten out of 100 to be removed in turn are selected by uniform random distribution. The average differences of KL divergence between the normal data and the polluted data for each case are drawn in Fig. 6. Regardless of the SP number variation, Case 2 and Case 4 have similar the average differences of KL divergences. This can be validated from that the KL divergences of the polluted data have the almost same KL values of normal data, as shown in Figs. 4(b) and 4(d). On the other hand, Cases 1 and 3 are

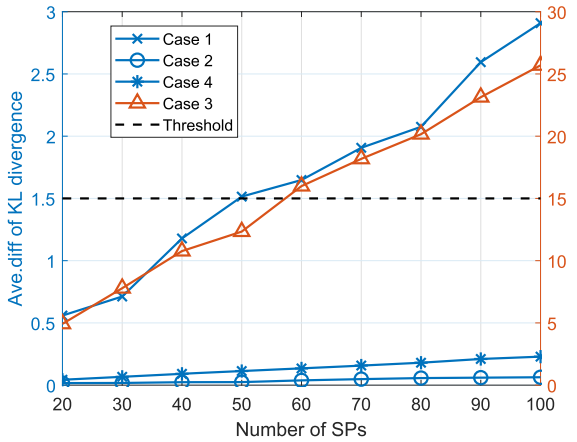

Fig. 6. Average difference (Ave.diff) of KL divergences of Cases 1∼4 with respect to the variation of SP numbers. To meet the setup of threshold value 1.5 defined in Fig. 4, which triggers the detection moment, it requires more than 50 number of SPs.

majorly-changing scenarios, and the average differences of KL divergences are decreasing with respect to the decrement of the SP numbers. In this paper, we set 1.5 ave.diff value as the threshold so that the required SP numbers to work for

the desired change detection confirmed in Fig. 4 are more than 50.

V. Conclusion

This paper presents a new change detection algorithm for the situation where RSSI fingerprint pattern is changed compared to an initial RSSI fingerprint database. The comparison mechanism is built by the feature database reconstruction and the KL divergence calculation. When we test the polluted data compared with the normal data, the developed algorithm accurately recognized the similarity between the polluted data and the normal data.

References

[1] S.-H. Fang, W.-H. Chang, Y. Tsao, H.-C. Shih, and C. Wang, "Channel state reconstruction using multilevel discrete wavelet transform for improved fingerprinting-based indoor localization," *IEEE Sensors J.*, vol. 16, no. 21, pp. 7784–7791, Nov. 1, 2016.

[2] M. T. Hoang *et al.*, "A soft range limited k-nearest neighbors algorithm for indoor localization enhancement," *IEEE Sensors J.*, vol. 18, no. 24, pp. 10208–10216, Dec. 15, 2018.

[3] W. Xue, W. Qiu, X. Hua, and K. Yu, "Improved Wi-Fi RSSI measurement for indoor localization," *IEEE Sensors J.*, vol. 17, no. 7, pp. 2224–2230, Apr. 1, 2017.

[4] A. R. J. Ruiz, F. S. Granja, J. C. P. Honorato, and J. I. G. Rosas, "Accurate pedestrian indoor navigation by tightly coupling foot-mounted IMU and RFID measurements," *IEEE Trans. Instrum. Meas.*, vol. 61, no. 1, pp. 178–189, Jan. 2012.

[5] Y. Zhao *et al.*, "Estimation of pedestrian altitude inside a multi-story building using an integrated micro-IMU and barometer device," *IEEE Access*, vol. 7, pp. 84680–84689, 2019.

[6] E. Brachmann and C. Rother, "Learning Less Is More—6D camera localization via 3D surface regression," in *Proc. IEEE Conf. Comput. Vis. Pattern Recognit.*, Jun. 2018, pp. 4654–4662.

[7] W. Elloumi, A. Latoui, R. Canals, A. Chetouani, and S. Treuillet, "Indoor pedestrian localization with a smartphone: A comparison of inertial and vision-based methods," *IEEE Sensors J.*, vol. 16, no. 13, pp. 5376–5388, Jul. 2016.

[8] G. Wang, X. Wang, J. Nie, and L. Lin, "Magnetic-based indoor localization using smartphone via a fusion algorithm," *IEEE Sensors J.*, vol. 19, no. 15, pp. 6477–6485, Aug. 1, 2019.

[9] Y. Shu, C. Bo, G. Shen, C. Zhao, L. Li, and F. Zhao, "Magicol: Indoor localization using pervasive magnetic field and opportunistic WiFi sensing," *IEEE J. Sel. Areas Commun.*, vol. 33, no. 7, pp. 1443–1457, Jul. 2015.

[10] Y. Shu *et al.*, "Gradient-based fingerprinting for indoor localization and tracking," *IEEE Trans. Ind. Electron.*, vol. 63, no. 4, pp. 2424–2433, Apr. 2016.

[11] J. Y. Zhu, A. X. Zheng, J. Xu, and V. O. Li, "Spatio-temporal (S-T) similarity model for constructing WIFI-based RSSI fingerprinting map for indoor localization," in *Proc. Int. Conf. Indoor Positioning Indoor Navigat.*, Oct. 2014, pp. 678–684.

[12] S. Ezpeleta, J. Claver, J. Pérez-Solano, and J. Martí, "RF-based location using interpolation functions to reduce fingerprint mapping," *Sensors*, vol. 15, no. 10, pp. 27322–27340, Oct. 2015.

[13] H. Zou, Y. Zhou, H. Jiang, B. Huang, L. Xie, and C. Spanos, "Adaptive localization in dynamic indoor environments by transfer kernel learning," in *Proc. IEEE Wireless Commun. Netw. Conf.*, Mar. 2017, pp. 1–6.

[14] S. J. Pan, V. W. Zheng, Q. Yang, and D. H. Hu, "Transfer learning for WiFi-based indoor localization," in *Proc. Assoc. Advancement Artif. Intell. (AAAI) Workshop*, vol. 6, Jul. 2008, pp. 1–6.

[15] Z. Sun, Y. Chen, J. Qi, and J. Liu, "Adaptive localization through transfer learning in indoor Wi-Fi environment," in *Proc. 7th Int. Conf. Mach. Learn. Appl.*, Dec. 2008, pp. 331–336.

[16] M. Zhou, Y. Tang, W. Nie, L. Xie, and X. Yang, "GrassMA: Graph-based semi-supervised manifold alignment for indoor WLAN localization," *IEEE Sensors J.*, vol. 17, no. 21, pp. 7086–7095, Nov. 2017.

[17] M. Zhou, Y. Tang, Z. Tian, L. Xie, and W. Nie, "Robust neighborhood graphing for semi-supervised indoor localization with light-loaded location fingerprinting," *IEEE Internet Things J.*, vol. 5, no. 5, pp. 3378–3387, Oct. 2017.

[18] J. Yoo and H. Kim, "Target localization in wireless sensor networks using online semi-supervised support vector regression," *Sensors*, vol. 15, no. 6, pp. 12539–12559, May 2015.

[19] M. Mohammadi, A. Al-Fuqaha, M. Guizani, and J. Oh, "Semisupervised deep reinforcement learning in support of IoT and smart city services," *IEEE Internet Things J.*, vol. 5, no. 2, pp. 624–635, Apr. 2018.

[20] Y. Gu, Y. Chen, J. Liu, and X. Jiang, "Semi-supervised deep extreme learning machine for Wi-Fi based localization," *Neurocomputing*, vol. 166, pp. 282–293, Oct. 2015.

[21] Z. E. Khatab, A. Hajihoseini, and S. A. Ghorashi, "A fingerprint method for indoor localization using autoencoder based deep extreme learning machine," *IEEE Sensors Lett.*, vol. 2, no. 1, Mar. 2017, Art. no. 6000204.

[22] J. Yoo, K. H. Johansson, and H. J. Kim, "Indoor localization without a prior map by trajectory learning from crowdsourced measurements," *IEEE Trans. Instrum. Meas.*, vol. 66, no. 11, pp. 2825–2835, Nov. 2017.

[23] J. Niu, B. Wang, L. Cheng, and J. J. P. C. Rodrigues, "WicLoc: An indoor localization system based on WiFi fingerprints and crowdsourcing," in *Proc. IEEE Int. Conf. Commun.*, Jun. 2015, pp. 3008–3013.

[24] Q. Jiang, Y. Ma, K. Liu, and Z. Dou, "A probabilistic radio map construction scheme for crowdsourcing-based fingerprinting localization," *IEEE Sensors J.*, vol. 16, no. 10, pp. 3764–3774, May 15, 2016.

[25] S.-H. Fang and T. Lin, "Principal component localization in indoor WLAN environments," *IEEE Trans. Mobile Comput.*, vol. 11, no. 1, pp. 100–110, Jan. 2012.

[26] D. Li, B. Zhang, and C. Li, "A feature-scaling-based k-nearest neighbor algorithm for indoor positioning systems," *IEEE Internet Things J.*, vol. 3, no. 4, pp. 590–597, Aug. 2015.

[27] X. Jiang, Y. Chen, J. Liu, Y. Gu, and L. Hu, "FSELM: Fusion semi-supervised extreme learning machine for indoor localization with Wi-Fi and Bluetooth fingerprints," *Soft Comput.*, vol. 22, no. 11, pp. 3621–3635, Jun. 2018.

[28] I. Jolliffe, *Principal Component Analysis*. New York, NY, USA: Springer, 2011.

[29] L. Csató and M. Opper, "Sparse on-line Gaussian processes," *Neural Comput.*, vol. 14, no. 3, pp. 641–668, Mar. 2002.

[30] D. J. MacKay and D. J. Mac Kay, *Information Theory, Inference and Learning Algorithms*. Cambridge, U.K.: Cambridge Univ. Press, 2003.

[31] S. B. Kang, N. Joshi, C. L. Zitnick, T. S. Cho, R. Szeliski, and W. T. Freeman, "Image restoration by matching gradient distributions," *IEEE Trans. Pattern Anal. Mach. Intell.*, vol. 34, no. 4, pp. 683–694, Apr. 2012.

[32] D. Yu, K. Yao, H. Su, G. Li, and F. Seide, "KL-divergence regularized deep neural network adaptation for improved large vocabulary speech recognition," in *Proc. IEEE Int. Conf. Acoust., Speech Signal Process.*, May 2013, pp. 7893–7897.

[33] O. Abdullah, "Convex optimization via symmetrical Hölder divergence for a WLAN indoor positioning system," *Entropy*, vol. 20, no. 9, p. 639, Aug. 2018.

[34] P. Mirowski, H. Steck, P. Whiting, R. Palaniappan, M. MacDonald, and T. K. Ho, "KL-divergence kernel regression for non-Gaussian fingerprint based localization," in *Proc. Int. Conf. Indoor Positioning Indoor Navigat.*, Sep. 2011, pp. 1–10.

[35] D. Milioris, L. Kriara, A. Papakonstantinou, G. Tzagkarakis, P. Tsakalides, and M. Papadopouli, "Empirical evaluation of signal-strength fingerprint positioning in wireless LANs," in *Proc. ACM Int. Conf. Modeling, Anal., Aimulation Wireless Mobile Syst.*, Oct. 2010, pp. 5–13.

[36] K. Wang *et al.*, "Learning to improve WLAN indoor positioning accuracy based on DBSCAN-KRF algorithm from RSS fingerprint data," *IEEE Access*, vol. 7, pp. 72308–72315, 2019.

Jaehyun Yoo (S'14–M'17) received the B.S. degree in information and control engineering, Kwangwoon University, Seoul, South Korea, in 2010, and the M.S and Ph.D. degrees from the School of Mechanical and Aerospace Engineering, Seoul National University, Seoul, in 2016. He was a Postdoctoral Researcher with the School of Electrical Engineering and Computer Science, KTH Royal Institute of Technology, Stockholm, Sweden. He is a Professor with the Electrical, Electronic and Control Department, Hankyong National University. His research interests include machine learning, event-triggered automatic control, indoor localization, and robotic systems.